Available online at www.sciencedirect.com
ScienceDirect
Physics Procedia 70 (2015) 1216 – 1220
Physics Procedia

2015 International Congress on Ultrasonics, 2015 ICU Metz

High Frame Rate Super Resolution Imaging Based on Ultrasound Synthetic Aperture Scheme

Takayuki Wada[a], Yihsin Ho[a], Kan Okubo[a], Norio Tagawa[a,*], Yoshiyasu Hirose[b]

[a] Graduate School of System Design, Tokyo Metropolitan University, 6-6 Asahigaoka, Hino-shi, Tokyo 191-0065, Japan
[b] ITOCHU Techno-Solutions Corporation, 3-2-5 Kasumigaseki, Chiyoda-ku, Tokyo 100-6080, Japan

Abstract

This study addresses the efficient extension of the Super resolution FM-Chirp correlation Method (SCM) to the framework of synthetic aperture imaging. The original SCM needs to transmit focused beams many times while changing frequency little by little toward each direction to extract the carrier phase information which is useful for super resolution imaging. This multiple transmitting and receiving increase the amount of processing and puts a strict limit on the frame rate. Therefore, we extend the SCM to the synthetic aperture version called the SA-SCM, and confirm its performance through simulations based on the finite element method.

Peer-review under responsibility of the Scientific Committee of ICU 2015

Keywords: ultrasound imaging; super resolution; synthetic aperture; high frame rate; FM-chirp; pulse compression; MUSIC

1. Introduction

In order to perform high resolution ultrasound imaging, we have already proposed a Super resolution FM-Chirp correlation Method (SCM) through Fujiwara et al. [1]. The SCM is based on the MUSIC (MUltiple SIgnal Classification) algorithm introduced by Schmidt [2], which is proposed as a direction-of-arrival estimation method for electrical waves. Although, in principle, the SCM method can use any signal as a transmission pulse, an FM-chirp signal can be effectively used for obtaining high SNR images by adopting the pulse compression technique (PCT).

In the SCM, multiple transmissions of an ultrasound pulse with slightly different frequency-band are required for generating each line in an image. This increases the amount of processing and puts a strict limit on a frame rate. On the other hand, studies for synthetic aperture imaging (SAI) are being vigorously advanced [3]. SAI can perform high frame-rate imaging, and hence, it is useful for improvement of accuracy in diagnosis of a heart disease and its various modifications for high-performance are examined. The compressed sensing strategy, which is recently receiving a lot of attention, is adopted to improve the frame-rate of SAI furthermore by several studies, for example [4]. In this study, we attempt to solve the above mentioned multiple transmissions problem through the application of SAI. We introduce the synthetic aperture version of the SCM called the SA-SCM. The time required for the SCM imaging can

* Corresponding author. Tel.: +81-42-585-8416 ; fax: +81-42-583-5119.
E-mail address: tagawa@tmu.ac.jp

1875-3892
Peer-review under responsibility of the Scientific Committee of ICU 2015
doi:10.1016/j.phpro.2015.08.262

be reduced by the synthetic aperture technique, but image degradation is concerned, because the incoherence of the carrier wave may stand out by delay-and-sum beam forming using a wide aperture. We examine the degree of such the degradation of the SA-SCM through finite element method (FEM) simulations.

2. Method

2.1. Outline of super resolution FM-chirp correlation method

In this section, we review how the SCM employs MUSIC to get super resolution along a range direction in imaging. We receive an echo signal $y(t)$ in the RF-band from D scatterers against a transmitted FM-chirp signal $s(t) = \mathrm{Re}[x(t)e^{j\omega_0 t}]$ having the center frequency of ω_0 as follows:

$$y(t) = \int_{-\infty}^{\infty} h(\tau)s(t-\tau)d\tau, \qquad h(t) = \sum_{i=1}^{D} h_i\delta(t-\tau_i), \tag{1}$$

where $h(t)$ is the impulse response, $\{\tau_i\}$ is a set of propagation delays that should be estimated, and $\delta(\cdot)$ is the Dirac delta function. The received echo expressed as an analytic signal in the base-band indicated by $v(t)$ and the compressed signal of $v(t)$ indicated by $z(t)$ are formulated as follows:

$$v(t) = \sum_{i=1}^{D} h_i x(t-\tau_i)e^{-j\omega_0\tau_i} + n(t), \qquad z(t) = \sum_{i=1}^{D} h_i e^{-j\omega_0\tau_i} r(t-\tau_i) + m(t), \tag{2}$$

where $r(t)$ is the complex-valued auto-correlation function of $x(t)$, which is the base-band modulation signal, and $z(t)$ is the complex-valued delay profile. We suppose that the noise $n(t)$ is generated by the Gaussian white noise process with a variance of σ^2, and hence, $m(t)$ is the complex-valued cross-correlation of $x(t)$ with $n(t)$. As the discrete representation, we define a compressed echo vector in the base-band $\mathbf{z} \equiv [z(t_1), z(t_2), \cdots, z(t_M)]^\top$, a steering vector $\mathbf{r}_i \equiv [r(t_1-\tau_i), r(t_2-\tau_i), \cdots, r(t_M-\tau_i)]^\top$ and a noise vector $\mathbf{m} \equiv [m(t_1), m(t_2), \cdots, m(t_M)]^\top$ with the number of time sampling M. In terms of the array manifold matrix $\mathbf{\Gamma} \equiv [\mathbf{r}_i, \mathbf{r}_2, \cdots, \mathbf{r}_D]$ and the gain vector $\mathbf{g} \equiv [h_1 e^{-j\omega_0 t_1}, h_2 e^{-j\omega_0 t_2}, \cdots, h_D e^{-j\omega_0 t_D}]^\top$, $\mathbf{z}$ and its variance-covariance matrix $\mathbf{R} \equiv E\{\mathbf{z}\mathbf{z}^{\mathrm{H}}\}$ can be represented as follows:

$$\mathbf{z} = \Gamma\mathbf{g} + \mathbf{m}, \qquad \mathbf{R} = \mathbf{\Gamma}\mathbf{G}\mathbf{\Gamma}^{\mathrm{H}} + \mathbf{R}_n, \tag{3}$$

where $\mathbf{G} \equiv E\{\mathbf{g}\mathbf{g}^{\mathrm{H}}\}$ and $\mathbf{R}_n \equiv E\{\mathbf{m}\mathbf{m}^{\mathrm{H}}\} = \sigma^2\mathbf{R}_0$, in which $\mathbf{R}_0$ is the Hermitian matrix whose klth element is $r(t_k - t_l)$. The SCM relies on the generalized eigenvalue decomposition having the following form:

$$\mathbf{R}\mathbf{e}_i = \lambda_i\mathbf{R}_0\mathbf{e}_i : \qquad i = 1, 2, \cdots, M. \tag{4}$$

Under the condition that $M > D$, the columns of $\mathbf{\Gamma}$ are linearly independent, the rank of $\mathbf{R} - \mathbf{R}_n = \mathbf{\Gamma}\mathbf{G}\mathbf{\Gamma}^{\mathrm{H}}$ is D, and therefore $\mathbf{R}$ has D generalized eigenvalues greater than σ^2 and $M - D$ eigenvalues equal to σ^2. The set of D eigenvectors $\{\mathbf{e}_i\}_{i=1}^{D}$ corresponding to the largest D eigenvalues span the signal subspace, and the residual $M - D$ eigenvectors $\{\mathbf{e}_i\}_{i=D+1}^{M}$ span the subspace which includes no signals and is called the noise subspace. The noise subspace is orthogonal to the steering vectors evaluated at the true delays. For estimating the true delays, we can use the orthogonality between the steering vector and the noise subspace while varying the delay of the steering vector. Based on the MUSIC algorithm, a super-resolution delay profile $S(t_i)$ might be defined as follows:

$$S(t_i) \equiv \frac{\mathbf{r}_i^{\mathrm{H}}\mathbf{R}_0^{-1}\mathbf{r}_i}{\sum_{j=D+1}^{M}|\mathbf{r}_i^{\mathrm{H}}\mathbf{e}_j|^2}. \tag{5}$$

D should correspond to the number of target signals in the echo, and in actual applications, for example the Akaike's Information Criterion (AIC) or the Minimum Description Length (MDL) criterion is used for determining D. To estimate $\mathbf{R}$ by avoiding that the rank of $\mathbf{\Gamma}\mathbf{G}\mathbf{\Gamma}^{\mathrm{H}}$ is reduced to 1, which may be caused because of the path coherence, we can adopt the random frequency smoothing method. This SCM sweeps the frequency-band of the transmission randomly in the appropriate range so as to vary the carrier phase at each sampling time in the compressed echo from $-\pi$ to $+\pi$. With K times transmissions having a randomly shifted frequency-band, we estimate $\mathbf{R}$ as $\hat{\mathbf{R}} = (\sum_{k=1}^{K}\mathbf{z}_k\mathbf{z}_k^{\mathrm{H}})/K$, where $\mathbf{z}_k$ indicates the compressed base-band echo vector for the ith transmission.

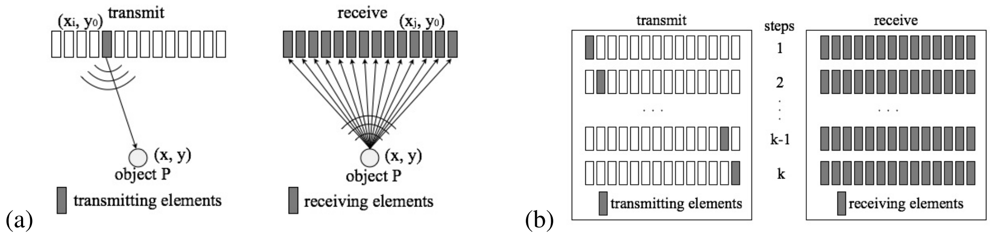

Fig. 1. Schematic of SAI: (a) state of transmitting (left image) and receiving (right image); (b) assignment patterns of transmitting (left image) and receiving (right image) elements in each imaging step.

2.2. Outline of synthetic aperture imaging

The simple SAI transmits ultrasonic waves towards a wide-range region from one transmitting element as shown in the left part of Fig. 1(a), and the echo reflected from an object P is received by all elements for imaging as shown in the right part of Fig. 1(a). Dynamic focusing is done as a delay-and-sum beam forming using the distance from a transmitting element to an imaging point and back to a receiving element. Dividing this distance by the speed of sound c gives the delay time t_k to extract proper signals. For the imaging point $P(x, y)$ shown in Fig. 1(a), the delay time is calculated as

$$t_k = \frac{\sqrt{(x_i - x)^2 + (y_0 - y)^2} + \sqrt{(x_j - x)^2 + (y_0 - y)^2}}{c}, \tag{6}$$

where (x_i, y_0) denotes the position of the transmitting element i and (x_j, y_0) is the position of the receiving element j. For each transmission, the beam forming is performed for every imaging point, and a low-SNR image is obtained. The transmitting element for each imaging step is changed as shown in the left image in Fig. 1(b), and echoes are received generally by all elements. By combining low-SNR images, the image with higher SNR can be obtained. To increase the emitted power and relax the limit of penetration depth generally caused by the transmission of un-focused waves, a sub-aperture consisting of several adjacent elements can be used for each transmission simultaneously [5], which is adopted in this study.

2.3. Extension of SCM to synthetic aperture scheme

The above mentioned SCM performs a super resolution processing for every imaging line. Therefore, multiple FM chirp pulses with slightly shifting a frequency-band are required to be transmitted toward each direction corresponding to each imaging line. It makes acquisition of moving images difficult. In SAI, an unfocused pulse is transmitted, and echoes from whole imaging region can be received through only one transmission. By randomly shifting a frequency-band of each transmitted FM chirp pulse in SAI, we can reduce the total number of the transmissions. We call the extended SCM using the SAI scheme the SA-SCM hereafter. The SCM with N imaging lines and K times transmissions needs $N \times K$ times transmissions for performing whole imaging, but the SA-SCM needs only K times.

To avoid a frequency bias related to the position of the sub-aperture for the transmission, we assign the frequency-band of the transmission randomly to the position of the sub-aperture. The SCM algorithm uses the phase information of a carrier wave along with an imaging line for super resolution imaging. The carrier wave included in the compressed echo corresponding to the imaging line for the SA-SCM may be corrupted by the delay-and-sum beam forming, which lowers the performance of super resolution.

3. Performance evaluation through simulations

3.1. Simulation set-up

We examined the performance of the proposed SA-SCM through simulations using PZFlex (Weidlinger Associates), which is a standard finite element method (FEM) code for ultrasound propagation. Figure 2(a) shows the

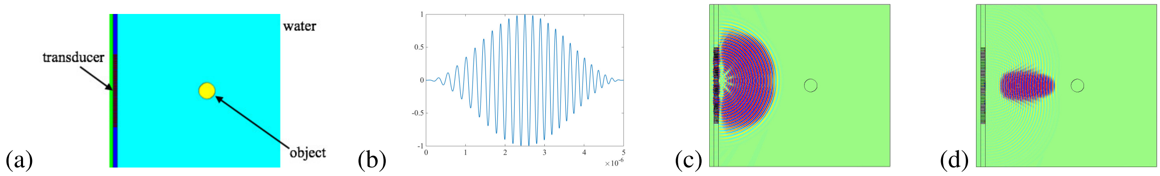

Fig. 2. Simulation conditions: (a) simulation model; (b) transmission wave (FM-chirp signal with Hanning window); (c) propagation of unfocused beam; (d) propagation of focused beam.

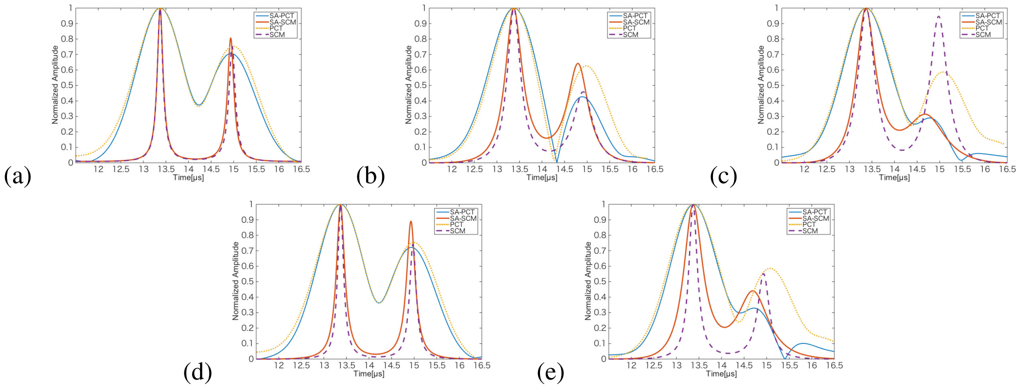

Fig. 3. Results of cross-sectional image profile along horizontal line passing through target: (a) array of 36 elements with transmissions of 29 times; (b) array of 64 elements with transmissions of 29 times; (c) array of 96 elements with transmissions of 29 times; (d) array of 36 elements with transmissions of 15 times; (e) array of 96 elements with transmissions of 45 times.

simulation model, in which water is used as a propagation medium and a target object with 1.5 mm of a diameter, 900 kg/m^3 of a density and 2000 m/s of a sound speed is placed 10 mm away from a transducer. We suppose a linear array transducer model in which the width of an element and a spacer is 0.08 mm and 0.06 mm respectively.

A transmission wave emitted toward a wide imaging region is formed by a sub-aperture consisting of 8 elements each of which is driven by a FM-chirp signal with the Hanning window shown in Fig. 2(b), and an echo from the target object is received by all elements. The specification of the transmitted FM-chirp signal is that a center frequency of 5 MHz, a band width of 2 MHz and a pulse duration of 5 μs. An example of the simulated propagation process of an unfocused wave for SAI is shown in Fig. 2(c). The beam focused on the object position and used to evaluate the conventional SCM is transmitted by all elements composing the array as shown in Fig. 2(d).

3.2. Simulation results

We evaluated the influence of the aperture width on the SA-SCM's wave form. By changing the number of the elements in the transducer as 36, 64 and 96, i.e., the aperture width of 4.98, 8.90 and 13.38 mm respectively, we simulated the SA-PCT and the SA-SCM. For a comparison, the PCT imaging and the SCM using a focused beam were also evaluated. The number of transmissions with different frequency-band for estimate $\hat{\mathbf{R}}$ is fixed as 29, and the frequency-band is randomly shifted between the range from 3 MHz to 7 MHz. In SAI, the sub-aperture for transmission consisting of 8 elements was located every equality in the aperture, and the echo is received by all elements. For the focused beam imaging, i.e., the usual PCT and the SCM, all elements were used for both of transmitting and receiving in all transducers having a different aperture width. Additionally, to check the effectiveness of the estimate of $\mathbf{R}$, i.e., the estimate of the signal subspace, we changed the number of transmissions.

The results are shown in Fig. 3 as a 1-D cross-sectional profile along the horizontal center line passing through the object in Fig. 2(a). Figures 3(a), (b) and (c) indicate the results by changing the aperture width, i.e., the number of elements composing the array, with fixing the transmissions of 29. From these, the performance of the usual PCT using a focused beam hardly depends on the aperture width, but in the results of the SA-PCT we can confirm that the

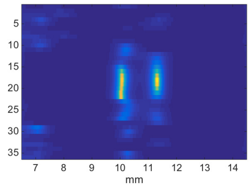

(a)

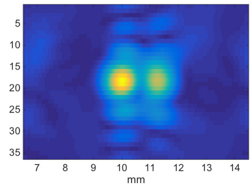

(b)

Fig. 4. Results of 2-D images consisting of 8 lines by array of 36 elements with transmissions of 15: (a) SA-SCM; (b) SA-PCT.

echo from the back face of the target becomes extremely small as the aperture becomes wide, although that from the front face is almost invariant with respect to the aperture width. As for the reason, it is thought that the incoherence of the echo stands out by the diffraction caused by the target's front face, which is hard to occur for a focused beam. Since, in this study, the pulse compression is processed after the delay-and-sum beam forming, such a incoherence causes the deterioration of the compressed wave form severely. The lowering of the SA-SCM performance according to the widening of the aperture can be explained also as a result of the incoherence. For the resulted signals from the front face of the target shown in Fig. 3(a), (b) and (c), it is known that the performances of the SCM and the SA-SCM are almost the same. It means that the SA-SCM functions correctly in the case that the SA-PCT can be applied effectively.

In addition, Fig. 3(d) shows the result by the same element number of 36 with Fig. 3(a) but using 15 times transmissions which is smaller than Fig. 3(a). Figure 3(e) corresponds to the result by 96 elements array using 45 times transmissions which is larger than Fig. 3(c). By comparing Fig. 3(a) and (d), we can confirm that much information of the signal subspace makes the performance of both the SCM and the SA-SCM improved if the aperture width is small. However, by comparing Fig. 3(c) and (e) with focusing on the signals from the front face, for the wide aperture the effectiveness of the increase of the transmissions' number is different between the SCM and the SA-SCM. This phenomena indicates that multiple transmissions along the same direction is better than those along various directions, which will have to be examined in detail in future. Figure 4 shows the 2-D images obtained by the SA-SCM and the SA-PCT by the array of 36 elements using 15 times transmissions. The range resolution is apparently improved by adopting the SCM algorithm but the azimuth resolution is unchanged.

4. Conclusions

In this study, we extended the SCM to SAI as the SA-SCM so as to improve the efficiency of the SCM and to realize the super resolution imaging with a high frame rate. Through the FEM simulations, the echo's coherency of SAI is important for the high performance of the SA-SCM. Additionally, it was confirmed that the multiple transmissions which is the key technique of the SCM algorithm are desired to be done from the same direction. This qualification is disadvantageous for the SA-SCM, and its solution should be examined. The azimuth resolution should be simultaneously improved in future.

Acknowledgements

This work was supported by JSPS KAKENHI Grant Number 25350569.

References

[1] Fujiwara M, Okubo K, Tagawa N. A Novel Technique for High Resolution Ultrasound Super Resolution FM-Chirp Correlation Method (SCM). *Proc. IEEE International Ultrasonics Symposium* 2009; 2390–2393.

[2] Schmidt RO. Multiple Emitter Location and Signal Parameter Estimation. *IEEE Trans. Antennas and Propagation* 1986; 34:276–280.

[3] Jensen JA, Nikolov SI, Gammelmark KL, Pedersen MH. Synthetic Aperture Ultrasound Imaging. *Ultrasonics* 2006; 44:e5–e15.

[4] Quinsac C, Basarab A, Girault J, Kouame D. Compressed Sensing of Ultrasound Images: Sampling of Spatial and Frequency Domains. *IEEE Workshop on Signal Processing Systems* 2010; 231-236.

[5] Karaman M, O'Donnell M. Subaperture Processing for Ultrasonic Imaging. *IEEE Trans. Ultrasonics, Ferroelectrics, and Frequency Control* 1998; 45:126–135.